Biochemical and Biophysical Research Communications **280,** 19–24 (2001)
doi:10.1006/bbrc.2000.4091, available online at http://www.idealibrary.com on IDEAL®

Structure Elucidation of Sphingolipids from the Mycopathogen *Sporothrix schenckii:* Identification of Novel Glycosylinositol Phosphorylceramides with Core Manα1→6Ins Linkage[1]

Marcos S. Toledo,* Steven B. Levery,†,[2] John Glushka,† Anita H. Straus,* and Helio K. Takahashi*,†,[2]

**Department of Biochemistry, Universidade Federal de São Paulo/Escola Paulista de Medicina, Rua Botucatu 862, 04023-900, São Paulo, SP, Brazil; and †Department of Biochemistry and Department of Molecular Biology, and Complex Carbohydrate Research Center, University of Georgia, 220 Riverbend Road, Athens, Georgia 30602*

Received November 30, 2000

Acidic glycosphingolipid components were extracted from the mycelium form of the thermally dimorphic mycopathogen *Sporothrix schenckii.* Two fractions from the mycelium form (Ss-M1 and Ss-M2), having the highest Rf values on HPTLC analysis, were isolated and their structures elucidated by 1- and 2-D ^{13}C- and ^{1}H-nuclear magnetic resonance spectroscopy, and electrospray ionization mass spectrometry with lithium adduction of molecular ions. The structures of Ss-M1 and Ss-M2 were determined to be Manα1→Ins1-P-1Cer and Manα1→3Manα1→Ins1-P-1Cer, respectively (where Ins = *myo*-inositol, P = phosphodiester). The Manα1→6Ins motif is found normally in diacylglycerol-based glycophosphatidylinositols of Mycobacteria, but this is the first unambiguous identification of the same linkage making up the core structure of fungal glycosylinositol phosphorylceramides (GIPCs). These results are discussed in relation to the structures of GIPCs of other mycopathogens, including *Histoplasma capsulatum* and *Paracoccidioides brasiliensis.*

Abbreviations used: Ins, *myo*-inositol; GIPC, glycosylinositol phosphorylceramide; NMR, nuclear magnetic resonance spectroscopy; TOCSY, total correlation spectroscopy; HMQC, heteronuclear multiple quantum correlation; HSQC, heteronuclear single quantum correlation; HMBC, heteronuclear multiple bond correlation; NOESY, nuclear Overhauser effect spectroscopy; HPLC, high performance liquid chromatography; HPTLC, high performance thin layer chromatography; ESI, electrospray ionization; MS, mass spectrometry; CID, collision-induced decomposition.

[1] This work was supported by FAPESP, CNPq, and PRONEX (Brasil; M.S.T., A.H.S., and H.K.T.); a Glycoscience Research Award from Neose Technologies, Inc. (S.B.L.); and the National Institutes of Health Resource Center for Biomedical Complex Carbohydrates (NIH No. 5 P41 RR05351; S.B.L. and J.G.).

[2] Address correspondence to either H.K.T. or S.B.L. E-mail: takahashi.bioq@epm.br or leverysb@ccrc.uga.edu.

The synthesis of glycosylinositol phosphorylceramides (GIPCs), a class of glycosphingolipids (GSLs) not found in mammalian cells, appears to be an essential requirement for the survival of fungi (4–6). Inhibitors of inositol phosphorylceramide (IPC) synthase, which catalyzes the obligatory first step in the biosynthetic pathway forming GIPCs from free ceramide, are highly toxic to many fungi but exhibit low toxicity in mammals (7–10). Thus, unlike inhibitors of enzymes responsible for ceramide biosynthesis, which affect mammals as well as fungi, IPC synthase inhibitors could potentially be useful as agents against disseminated mycosis in humans, an increasing threat paralleling the steady growth in populations of immunosuppressed or -compromised individuals (11). Inhibitors of later steps in the biosynthesis of GIPCs could also be useful, but the development of such agents will be accelerated by establishing an integrated model that includes detailed knowledge of the glycan structures expressed; the expression, regulation, and interactions of the glycosyltransferases responsible for their synthesis; and the possible functional significance of specific GIPC glycan structural features in the fungal repertoire. The development of immunodiagnostic agents directed against fungal GIPC glycans should also benefit from more detailed knowledge of the structures expressed and their distributions among various species with pathogenic potential.

With respect to mycopathogens, characterization of GIPCs from the Hemiascomycete *Candida albicans* have been carried out, although unambiguous confirmation of some structural details have not yet been published. More detailed structural characterization of GIPC antigens, linked to their specific immunological recognition in humans, have been published only for

0006-291X/01 $35.00

the thermally dimorphic Euascomycetes *Histoplasma capsulatum* (1, 12) and *Paracoccidioides brasiliensis* (13), which are closely related to each other. So far, GIPCs from these fungi have been characterized by a common core structure, Manα1→2Ins1-P-1Cer.[3] We have undertaken structure elucidation of GIPCs from the mycopathogen *Sporothrix schenckii*, which is also a thermally dimorphic Euascomycete, but is taxonomically more distant. In studying acidic components from the mycelium form of *S. schenckii*, we encountered GIPCs with a core linkage, Manα1→6Ins, not previously described in any sphingolipid structures. Characterization of these novel components is described herein.[4]

EXPERIMENTAL

Fungal isolate and growth conditions. The culture of *Sporothrix schenckii*, strain 65 (originally obtained from cutaneous footpad lesion of an otherwise healthy individual), was provided by Dr. Olga Gompertz, Department of Cellular Biology, Universidade Federal de São Paulo/Escola Paulista de Medicina, São Paulo, SP, Brasil. The same strain was used in a study of *S. schenckii* cerebrosides (14). Mycelium forms of *S. schenckii* strain 65 were grown in brain-heart infusion (BHI; 37 grams/L water), incubated at 25°C, using 2.5 L Fernbach flasks in a shaker at 150 rpm. Mycelia were inactivated with 0.1% of thimerosal, and after 48 h were collected by filtration on Whatman no. 1 filter paper.

Solvents for extraction and anion exchange chromatography. Solvent A, isopropanol/hexane/water (55:20:25, v/v/v, upper phase discarded); solvent B, chloroform/methanol (2:1, v/v); solvent C, chloroform/methanol/water (30:60:8, v/v/v).

High performance thin layer chromatography. Analytical HPTLC was performed on silica gel 60 plates (E. Merck, Darmstadt, Germany) using chloroform/methanol/water (60:40:9 v/v/v, containing 0.002% w/v $CaCl_2$; solvent D) as mobile phase. Lipid samples were dissolved in solvent B and applied by streaking from 5 μL Micro-caps (Drummond, Broomall, PA). For analytical HPTLC, detection was made by Bial's orcinol reagent (orcinol 0.55% [w/v] and H_2SO_4 5.5% [v/v] in ethanol/water 9:1 [v/v]; the plate is sprayed and heated briefly to ~200-250°C).

Extraction and purification of glycosphingolipids. Extraction and purification of glycosphingolipids were carried out as described previously (15–17). Briefly, glycosphingolipids were extracted by homogenizing yeast or mycelium forms (25–35 g wet weight) in an Omnimixer (Sorvall Inc., Wilmington, DE), three times with 200 mL of solvent A, and twice with 200 mL of solvent B. The five extracts were pooled, dried on a rotary evaporator, dialyzed against water, lyophilized, resuspended in solvent C, and applied to a column of DEAE-Sephadex A-25 (Ac^- form). Neutral glycosphingolipids were eluted with five volumes of solvent C. Acidic glycosphingolipids were eluted with five volumes of 0.5 M sodium acetate in MeOH. The acidic fraction was dried, dialyzed exhaustively against deionized water, redried and further purified by repetitive preparative-scale HPLC (50 cm × 4.6 mm Sphereclone [Phenomenex, Torrance, CA] 10 μm porous spherical silica; elution with 2-propanol-hexane-water gradient from 55:40:5 to 55:25:20 over 120 min, then isocratic for 40 min; flow rate 0.5 mL/min; 80 × 1 mL fractions collected). The identity and purity of each fraction was assessed by analytical HPTLC as above.

^{1}H-Nuclear magnetic resonance spectroscopy. Samples of underivatized GIPC (~0.5–1.0 mg) were deuterium exchanged by repeated lyophilization from D_2O, and then dissolved in 0.5 mL DMSO-d_6/2% D_2O (18–20) for NMR analysis. 1-D ^{1}H-NMR; 2-D ^{1}H-^{1}H-TOCSY (21, 22), ^{1}H-detected, ^{13}C-decoupled, phase sensitive, gradient (23) ^{13}C-^{1}H-HSQC (24) and -HMBC (25, 26) experiments were performed at 35°C on a Varian Unity Inova 600 MHz spectrometer using standard acquisition software available in the Varian VNMR software package. One-bond C-1/H-1 coupling constants were measured using a 1-D variant of a standard ^{1}H-detected, gradient ^{13}C-^{1}H-HMQC experiment performed without ^{13}C decoupling. Proton-decoupled 1-D ^{13}C-NMR spectra were acquired by direct detection on a Varian Unity Inova 500 MHz spectrometer under identical conditions. Proton chemical shifts are referenced to internal tetramethylsilane (δ = 0.000 ppm), carbon chemical shifts to the center line of residual DMSO (set at δ = 39.82 ppm).

Electrospray ionization mass spectrometry. ESI-MS and tandem ESI-MS/CID-MS were performed in the positive ion mode with Li^+ adduction (27–29) on a PE-Sciex (Concord, Ontario, Canada) API-III spectrometer, using a standard IonSpray source (orifice-to-skimmer voltage [OR], 100–130 V or 180 V ["high OR"]; Ionspray voltage, 5 kV; interface temperature, 45°C) and sample introduction by direct infusion (3–5 μL/min) of GIPC samples dissolved (~20 ng/μL) in 100% MeOH. For generation of Li_2^+ adducts of GIPC molecular species, a solution of LiI (10 mM) in MeOH was added (29) until the observed ratio of $M \cdot Li_2^+$ to $M \cdot LiNa^+$ in $^+$ESI-MS profile mode was <95:5 (the final concentration of LiI was generally 3–6 mM). For precursor ion tandem $^+$ESI-MS/CID-MS experiments, appropriate product ions from collision induced dissociation in Q2 (with argon as collision gas) were selected in Q3, while the useful precursor mass range (starting from ~m/z 50 below the product m/z) was scanned in Q1 (m/z 0.2 steps). OR was set to 100–120 V, the collision gas temperature [CGT] = 380–400 [× 10^{12} molecules/cm^2], and collision energy was 80 eV. Other parameters were set to achieve a peak width at ½ height deemed sufficient to assign nominal masses to all peaks in the mass range of interest. In general, spectra represent summations of 10–30 scans for single analyzer profiles, and 30–100 scans for CID experiments. Nominal monoisotopic m/z values are used in the description of ESI-MS results.

RESULTS

HPTLC profile of S. schenckii mycelium form GIPCs. An HPTLC profile of GIPCs from the mycelium form of *S. schenckii* is shown in Fig. 1. Five bands were visible with orcinol staining, designated Ss-M1 through Ss-M5. Of these, the first three appeared to be major components, with decreasing amounts of Ss-M4 and Ss-M5. The five components were isolated by repetitive HPLC and subjected to preliminary analysis by 1-D ^{1}H-NMR. Of these, Ss-M1, -M2, and -M3 appeared to be sufficiently homogeneous with respect to glycan structure to carry out further detailed characterization, while Ss-M4 and -M5 were very complex, with insufficient material available to warrant further fractionation and analysis.

NMR spectroscopic analysis of Ss-M1, -M2, and -M3. Ss-M1. In Fig. 2A are reproduced relevant downfield sections of 1-D ^{1}H-NMR spectra of *S. schenckii* mycelium form acidic fraction Ss-M1. A spectrum of an

[3] Although the studies of Barr *et al.* (1) did not specify precisely the linkage between Man and Ins, but characterized it as Manα1→2/6Ins, we have accumulated strong evidence that the core linkage for the *H. capsulatum* GIPCs which they reported is Manα1→2Ins (Toledo, Levery, Straus, Takahashi, unpublished data).

[4] A preliminary description of these results has been presented in poster form (2).

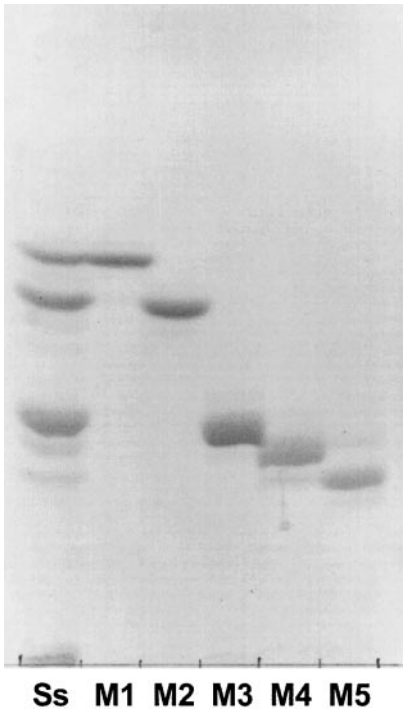

FIG. 1. HPTLC analysis comparing crude *S. schenckii* mycelium form GIPCs (lane Ss) with HPLC-purified fractions (lanes M1–M5). Relative concentration of components applied in lanes M4 and M5 was ~4–5× that in lanes M1–M3.

authentic Manα2IPC isolated from the mushroom *Agaricus blazei* was acquired under identical conditions for comparison (not shown). Differences were obvious in the chemical shifts of the anomeric proton signals (4.954 *versus* 5.041 ppm, respectively), as well as in observable resonances corresponding to *myo*-Ins H-5 and H-3, which in Manα2IPC were assigned at 2.956 and 3.222 ppm, respectively. Signals with the same splitting pattern are visible in the spectrum of Ss-M1 at 3.013 and 3.107 ppm, respectively. Chemical shift/connectivity assignments of all ^{1}H and ^{13}C signals, as well as approximate measurements of $^{3}J_{i,j}$ coupling constants, in the monosaccharide, inositol, and proximal part of the ceramide was performed by sequential application of 2-D ^{1}H-^{1}H COSY, ^{1}H-^{1}H TOCSY, and ^{1}H-^{13}C gHSQC NMR experiments (not shown). The chemical shift assignments for both compounds are listed in Table 1. All three residues in each compound were recognizable by their connectivity/coupling patterns. In particular, *myo*-Ins presents as a cyclic ^{1}H spin system in which all $^{3}J_{i,j}$ are large except for $^{3}J_{1,2}$ and $^{3}J_{2,3}$, as H-2 is the only equatorial proton in the 1,2,3,4,5,6-hexahydroxy-cyclohexane ring. The Man residue is also recognizable by its signature small values for $^{3}J_{1,2}$ and $^{3}J_{2,3}$; because $^{3}J_{1,2}$ is small for both the α- and β-anomeric configurations, it is difficult to distinguish between them under the conditions of this analysis. However, measurement of the one-bond H-1/C-1 coupling constant is decisive, this being in the range of 175–176 Hz in both cases; this is clearly too large for the β-configuration, for which the values are found in the range 160–165 Hz (30) (and references cited therein). With respect to linkage, particularly significant differences in the chemical shifts of signals corresponding to Ins C-2 and C-6 are diagnostic for the linkage →2Ins in the *A. blazei* Manα2IPC and →6Ins in Ss-M1; that is, a 6.6 ppm relative downfield shift of Ins C-2 in the Manα2IPC and a 6.1 ppm relative downfield shift of Ins C-6 in Ss-M1. The linkage assignments were confirmed by application of 2-D ^{1}H-^{1}H NOESY experiments, in which, at short mixing times (100 msec), interresidue correlations could only be observed between Man H-1 and Ins H-2 in Manα2IPC, and between Man H-1 and Ins H-6 in Ss-M1; and finally by application of 2-D ^{1}H-^{13}C gHMBC experiments, which established inter-residue connectivities unambiguously via observation of long-range (3-bond) transglycosidic correlations, Man H-1/Ins C-2 and Man C-1/Ins H-2 in Manα2IPC, and Man H-1/Ins C-6 and Man C-1/Ins H-6 in Ss-M1. The structure of Ss-M1 is thus clearly established as Manα6IPC.

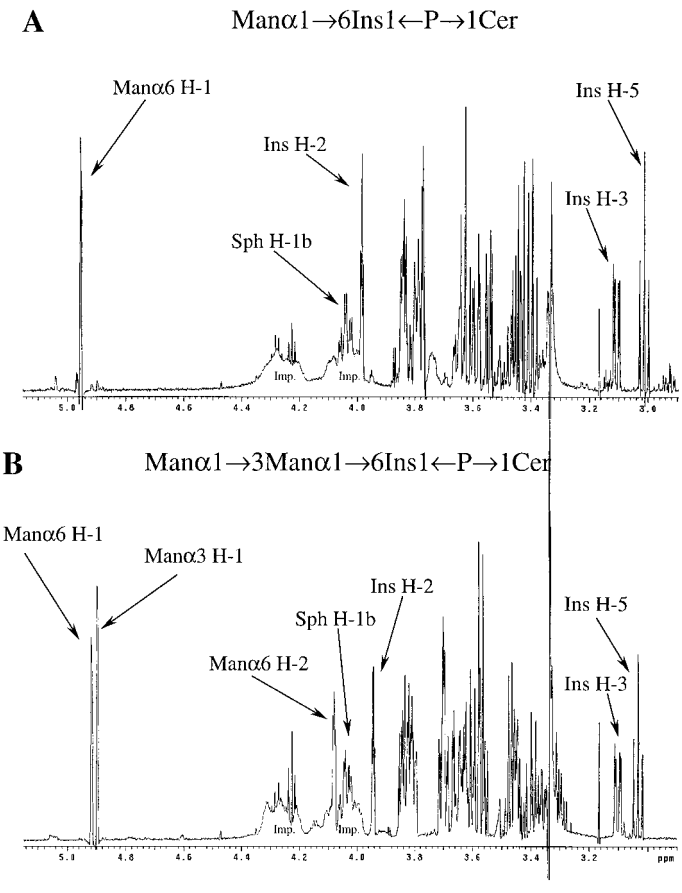

FIG. 2. Downfield sections of 1-D ^{1}H NMR spectra of GIPC fractions Ss-M1 (A) and Ss-M2 (B). Key reporter signals are marked. Imp., broad resonances from unidentified impurities.

TABLE 1

Comparison of ^{1}H and ^{13}C Chemical Shifts (ppm) for Monosaccharide, Inositol, Ceramide Sphingoid, and Fatty Acyl (in Parentheses) Residues of Manα6IPC from *Sporothrix schenckii* and Manα2IPC from *Agaricus blazei*, in DMSO-d_6/2% D_2O at 308°K (35°C)

	Manα1→6Ins1←P→1Cer			Manα1→2Ins1←P→1Cer		
H-1	4.954[a]	3.806	3.643, 4.040	5.041[b]	3.742	3.656, 4.048
H-2	3.772	3.984	3.838 (3.838)	3.696	3.965	3.839 (3.845)
H-3	3.544	3.107	3.435	3.510	3.222	3.470
H-4	3.099	3.395	3.365	3.468	3.341	3.360
H-5	3.785	3.013		3.851	2.956	
H-6	3.445	3.626		3.487	3.487	
H-6′	3.588			3.572		
C-1	101.25[c]	76.13	63.95 (173.42)	100.60[d]	75.71	64.05 (173.35)
C-2	70.14	71.18	50.38 (71.29)	70.35	77.84	50.35 (71.13)
C-3	71.05	71.16	73.12	70.71	70.44	72.82
C-4	67.50	72.69	70.44	66.70	72.11	70.35
C-5	73.32	73.79		72.82	75.49	
C-6	61.21	78.51		60.93	72.41	

[a] $^{3}J_{1,2}$ = 1.8 Hz.
[b] $^{3}J_{1,2}$ = 1.8 Hz.
[c] One-bond $^{1}J_{H\text{-}1,C\text{-}1}$ = 176 ± 1 Hz.
[d] One-bond $^{1}J_{H\text{-}1,C\text{-}1}$ = 175 ± 1 Hz.

Ss-M2. In a completely analogous way, the structure of Ss-M2 was established as Manα3Manα6IPC from analysis of its 1-D ^{1}H NMR spectrum (Fig. 2B), from complete assignments of relevant ^{1}H and ^{13}C resonances via 2-D spectroscopy (Table 2), and from NOESY and gHMBC through-space and through-bond correlation data. Thus in addition to the same set of Man/Ins correlations as given above for Ss-M1, interresidue correlations were observed connecting the second Man residue to the first, i.e., Man H-1/Man H-3 in the NOESY, Man C-1/Man H-3 and Man H-1/Man C-3 in gHMBC. Note the similarity in chemical shift of all ^{1}H and ^{13}C signals from the *myo*-Ins spin system, which are relatively unaffected by the glycosylation of the Man residue linked to it, especially the downfield shift of Ins C-6; in addition, C-3 of this Man residue is shifted downfield 6.3 ppm relative to its position in Ss-M1, the parent compound Manα6IPC.

TABLE 2

^{1}H and ^{13}C Chemical Shifts (ppm) for Monosaccharide, Inositol, Ceramide Sphingoid, and Fatty Acyl (in Parentheses) Residues of Manα3Manα6IPC from *Sporothrix schenckii* in DMSO-d_6/2% D_2O at 308°K (35°C)

	Manα1→3Manα1→6Ins1←P→1Cer			
H-1	4.898[a]	4.918[b]	3.814	3.644, 4.041
H-2	3.702	4.079	3.944	3.835 (3.848)
H-3	3.568	3.710	3.104	3.453
H-4	3.318	3.563	3.400	3.363
H-5	3.635	3.810	3.034	
H-6	3.382	3.467	3.607	
H-6′	3.673	3.585		
C-1	101.4[c]	101.8[d]	76.1	63.9
C-2	70.3	69.4	71.1	50.3 (71.26)
C-3	70.9	77.5	71.2	73.0
C-4	68.2	66.1	72.7	70.4
C-5	73.6	73.7	73.6	
C-6	61.7	61.2	79.3	

[a] $^{3}J_{1,2} < 2$ Hz.
[b] $^{3}J_{1,2} < 2$ Hz.
[c] One-bond $^{1}J_{H\text{-}1,C\text{-}1}$ = 171 ± 1 Hz.
[d] One-bond $^{1}J_{H\text{-}1,C\text{-}1}$ = 176 ± 1 Hz.

Ss-M3. From inspection of the 1-D ^{1}H NMR spectrum of Ss-M3 its structure was deduced as a triglycosyl-IPC with at least one β-linked sugar residue ($^{3}J_{1,2}$ = 7–9 Hz). Complete glycan structure elucidation by NMR spectroscopy, as was performed for Ss-M1 and -M2, established its structure as Manα3(Galβ4)Manα2IPC (data not shown). The complete analysis of this compound, the presence of which has also been observed in both morphological forms of *Histoplasma capsulatum* (12),[2] will be discussed in detail elsewhere (Toledo, Levery, Straus, and Takahashi, manuscript in preparation).

$^{+}$ESI-MS analysis of Ss-M1 and Ss-M2. Ss-M1. The major molecular ion species for Ss-M1 was observed in $^{+}$ESI-MS at *m/z* 1100 (not shown), consistent with a composition of Hex · Ins · P linked to Cer composed of t18:0 4-hydroxysphinganine (phytosphingosine) and h24:0 fatty acid. A number of other ions observed in this region were determined by tandem quadrupole $^{+}$ESI-MS/CID-MS experiments not to correspond to GIPC molecular species. At high OR, abundant fragments at *m/z* 417 and 690 were observed in the spectrum, corresponding to $[Hex \cdot Ins \cdot P \cdot Li_2]^{+}$

($[B_2PO_3 \cdot Li_2]^+$) and $[Cer \cdot Li]^+$ ($[Y_0 \cdot Li]^+$), respectively. Scanning for precursors of the ion *m/z* 417 showed that the only major molecular species in fraction Ss-M1 giving rise to that product was the one observed at *m/z* 1100. Related precursor molecular ions (5–10% of the abundance of *m/z* 1100) were also observed at *m/z* 1072, 1086, 1114, and 1128, corresponding to homologs of the major species differing by 1 or 2 CH_2 units more or less in either sphingosine or fatty acid; another ion in the cluster, at *m/z* 1084, would correspond to a minor molecular species missing one hydroxy group from the ceramide. Interestingly, a second cluster of precursor ions, in which the masses of all species differed from those in the first by +134 Th, was also observed; thus, the major species was found at *m/z* 1234, appearing at 15–20% of the abundance of *m/z* 1100. This implies that some additional moiety is attached to approximately 10% of Ss-M1.

Ss-M2. One major molecular ion species for Ss-M2 was observed in $^+$ESI-MS at *m/z* 1262, consistent with a composition of $Hex_2 \cdot Ins \cdot P$ linked to a Cer with the same composition as Ss-M1. At high OR, abundant fragments at *m/z* 417, 579 and 690 were observed in the spectrum, corresponding to $[Hex \cdot Ins \cdot P \cdot Li_2]^+$ ($[Y_2/B_3PO_3 \cdot Li_2]^+$), $[Hex_2 \cdot Ins \cdot P \cdot Li_2]^+$ ($[B_3PO_3 \cdot Li_2]^+$), and $[Cer \cdot Li]^+$ ($[Y_0 \cdot Li]^+$), respectively. Scanning for precursors of the ions *m/z* 579 and 417 showed that the only major molecular species in fraction Ss-M2 giving rise to these products was the one observed at *m/z* 1262. As with Ss-M1, a set of homologous related precursor ions (2–5% of the abundance of *m/z* 1396, again corresponding to some additional moiety 134 Th in mass, which appeared at 5–10% of the abundance of *m/z* 1262. The nature of this modification is currently under investigation.

DISCUSSION

In this work, preliminary characterization of GIPC structures in the mycopathogen *S. schenckii* revealed the unexpected expression of at least two varieties of glycan core structures, one of which has not been previously reported in fungi. These two variations contain either a Manα1→2Ins linkage, as previously reported, for example, in GIPCs of *P. brasiliensis* (13); or an isomeric Manα1→6Ins linkage, not previously reported in these components nor in any other sphingolipid reported so far.[5] Both linkages have been reported in glycosylinositol phosphorydiacylglycerols (phosphatidylinositol mannosides, or PIMs) of Mycobacteria (31). Previously, GIPCs of Basidiomycete fungi (*Agaricus* spp.) were reported to express GIPCs containing a Manβ1→2Ins core linkage (32); recently, however, new evidence has suggested that the core linkage in Basidiomycete GIPCs is instead also Manα1→2Ins (33), as shown, for example, by measurement of $^1J_{H\text{-}1,C\text{-}1}$ for the *A. blazei* MIPC used as a standard in this work. It is worth pointing out that reliance solely on the mass spectral evidence would have been insufficient in this case to differentiate between MIPCs containing Manα1→2Ins or Manα1→6Ins linkages. We hope that NMR data presented in this paper will be of use in identification and/or elucidation of structures of GIPCs from other fungi. In addition, precursor ion $^+$ESI-MS/CID-MS for obtaining clean molecular ion profiles for GIPC fractions, as demonstrated earlier by Jennemann *et al.* (33) in negative ion mode with selection of phosphate (*m/z* 79) in Q3, was found to be effective also in positive ion mode with selection of appropriate metalated fragment ions.

Clearly, the results in this study are only a preliminary step in determining any possible functional significance of such structures in *S. schenckii* or other fungi. While experiments with *S. cerevisiae* have begun to delineate some general functional roles for GIPCs (4, 5, 34, 35), which may be extrapolatable to other species, a picture of GIPC glycan structural diversity in the fungal kingdom is presently emerging which suggests the possibility of differing functions in some species. Recently, a putative gene (*SUR1*) for the UDP-Man:IPC Manα1→2 transferase has been identified in *S. cerevisiae* (36); inevitably either this or another gene will be verified to code for the active transferase, and the result will be extrapolated to other fungi, including mycopathogens. In attempts to correlate such putative genes with specific glycosyltransferase activities and their possible cellular functions, or to study potential interaction of fungal GSLs with the host immune system, we feel that awareness of the existence of alternate core linkages in fungal GIPCs will be an important experimental consideration.

[5] During preparation of the manuscript, an abstract appeared (3), in which structures of several GIPCs from the yeast form of *S. schenckii* were proposed to contain the Manα1→6Ins linkage.

REFERENCES

1. Barr, K., Laine, R. A., and Lester, R. L. (1984) Carbohydrate structures of three novel phosphoinositol-containing sphingolipids from the yeast *Histoplasma capsulatum. Biochemistry* **23,** 5589–5596.
2. Levery, S. B., Toledo, M. S., Doong, R. L., Fuller, M., Momany, M., Lindsey, R., Suzuki, E., Straus, A. H., and Takahashi, H. K. (2000) Comparative analysis of glycosylinositol phosphorylceramide and cerebroside expression in pathogenic and nonpathogenic fungi (Abstract #188). Proceedings of the 5th Annual Conference of the Society for Glycobiology, Boston, MA, 8–11 November 2000. *Glycobiology* **10,** 1128.
3. Penha, C. V. L., Lopes, L. M., Wait, R., Jones, C., Todeschini, A. R., Heise, N., Mendonca-Previato, L., and Previato, J. O. (2000) A novel family of glycophosphosphingolipid expressed by yeast forms of *Sporothrix schenckii:* evidence for a unique Manα1-6Ins-phosphorylceramide substructure (Abstract #176). Proceedings of the 5th Annual Conference of the Society for Glycobiology, Boston, MA, 8–11 November 2000. *Glycobiology* **10,** 1125.

4. Dickson, R. C., and Lester, R. L. (1999) Yeast sphingolipids. *Biochim. Biophys. Acta* **1426,** 347–357.
5. Dickson, R. C. (1998) Sphingolipid functions in *Saccharomyces cerevisiae:* Comparison to mammals. *Ann. Rev. Biochem.* **67,** 27–48.
6. Daum, G., Lees, N. D., Bard, M., and Dickson, R. (1998) Biochemistry, cell biology and molecular biology of lipids of *Saccharomyces cerevisiae. Yeast* **14,** 1471–1510.
7. Takesako, K., Kuroda, H., Inoue, T., Haruna, F., Yoshikawa, Y., and Kato, I. (1993) Biological properties of Aureobasidin A, a cyclic depsipeptide antifungal antibiotic. *J. Antibiot.* **49,** 1414–1420.
8. Nagiec, M. M., Nagiec, E. E., Baltisberger, J. A., Wells, G. B., Lester, R. L., and Dickson, R. C. (1997) Sphingolipid synthesis as a target for antifungal drugs. Complementation of the inositol phosphorylceramide synthase defect in a mutant strain of *Saccharomyces cerevisiae* by the *AUR1* gene. *J. Biol. Chem.* **272,** 9809–9817.
9. Mandala, S. M., Thornton, R. A., Rosenbach, M., Milligan, J., Garcia-Calvo, M., Bull, H. G., and Kurtz, M. B. (1997) Khafrefungin, a novel inhibitor of sphingolipid synthesis. *J. Biol. Chem.* **272,** 32709–32714.
10. Mandala, S. M., Thornton, R. A., Milligan, J., Rosenbach, M., Garcia-Calvo, M., Bull, H. G., Harris, G., Abruzzo, G. K., Flattery, A. M., Gill, C. J., Bartizal, S., and Kurtz, M. B. (1998) Rustmicin, a potent antifungal agent, inhibits sphingolipid synthesis at the inositol phosphoceramide synthase. *J. Biol. Chem.* **273,** 14942–14949.
11. Dixon, D. M., McNeil, M. M., Cohen, M. L., Gellin, B. G., and La, M. J. (1996) Fungal infections: A growing threat. *Public Health Rep.* **111,** 226–235.
12. Barr, K., and Lester, R. L. (1984) Occurrence of novel antigenic phosphoinositol-containing sphingolipids in the pathogenic yeast *Histoplasma capsulatum*. *Biochemistry* **23,** 5581–5588.
13. Levery, S. B., Toledo, M. S., Straus, A. H., and Takahashi, H. K. (1998) Structure elucidation of sphingolipids from the mycopathogen *Paracoccidioides brasiliensis:* An immunodominant β-galactofuranose residue is carried by a novel glycosylinositol phosphorylceramide antigen. *Biochemistry* **37,** 8764–8775.
14. Toledo, M. S., Levery, S. B., Straus, A. H., and Takahashi, H. K. (2000) Dimorphic expression of cerebrosides in the mycopathogen *Sporothrix schenckii. J. Lipid Res.* **41,** 797–806.
15. Toledo, M. S., Levery, S. B., Straus, A. H., Suzuki, E., Momany, M., Glushka, J., Moulton, J. M., and Takahashi, H. K. (1999) Characterization of sphingolipids from mycopathogens: Factors correlating with expression of 2-hydroxy fatty acyl (E)-Δ^3-unsaturation in cerebrosides of *Paracoccidioides brasiliensis* and *Aspergillus fumigatus. Biochemistry* **38,** 7294–7306.
16. Toledo, M. S., Suzuki, E., Straus, A. H., and Takahashi, H. K. (1995) Glycolipids from *Paracoccidioides brasiliensis.* Isolation of a galactofuranose-containing glycolipid reactive with sera of patients with paracoccidioidomycosis. *J. Med. Vet. Mycol.* **33,** 247–251.
17. Straus, A. H., Levery, S. B., Jasiulionis, M. G., Salyan, M. E., Steele, S. J., Travassos, L. R., Hakomori, S., and Takahashi, H. K. (1993) Stage-specific glycosphingolipids from amastigote forms of *Leishmania* (*L.*) *amazonensis.* Immunogenicity and role in parasite binding and invasion of macrophages. *J. Biol. Chem.* **268,** 13723–13730.
18. Dabrowski, J., Hanfland, P., and Egge, H. (1980) Structural analysis of glycosphingolipids by high-resolution ^{1}H nuclear magnetic resonance spectroscopy. *Biochemistry* **19,** 5652–5658.
19. Yamada, A., Dabrowski, J., Hanfland, P., and Egge, H. (1980) Preliminary results of *J*-resolved, two-dimensional ^{1}H-NMR studies on glycosphingolipids. *Biochim. Biophys. Acta* **618,** 473–479.
20. Dabrowski, J., Egge, H., and Hanfland, P. (1980) High resolution nuclear magnetic resonance spectroscopy of glycosphingolipids. I: 360 MHz ^{1}H and 90.5 MHz ^{13}C NMR analysis of galactosylceramides. *Chem. Phys. Lipids* **26,** 187–196.
21. Braunschweiler, L., and Ernst, R. R. (1983) Coherence transfer by isotropic mixing: Application to proton correlation spectroscopy. *J. Magn. Reson.* **53,** 521–528.
22. Bax, A., and Davis, D. G. (1985) MLEV-17-based two-dimensional homonuclear magnetization transfer spectroscopy. *J. Magn. Reson.* **65,** 355–360.
23. Davis, A. L., Keeler, J., Laue, E. D., and Moskau, D. (1992) Experiments for recording pure-absorption heteronuclear correlation spectra using pulsed field gradients. *J. Magn. Reson.* **98,** 207–216.
24. Bodenhausen, G., and Ruben, D. J. (1980) Natural abundance nitrogen-15 NMR by enhanced heteronuclear spectroscopy. *Chem. Phys. Lett.* **69,** 185–189.
25. Bax, A., and Summers, M. F. (1986) ^{1}H and ^{13}C assignments from sensitivity-enhanced detection of heteronuclear multiple-bond connectivity by 2D multiple quantum NMR. *J. Am. Chem. Soc.* **108,** 2093–2094.
26. Bax, A., and Marion, D. (1988) Improved resolution and sensitivity in ^{1}H-detected heteronuclear multiple-bond correlation spectroscopy. *J. Magn. Reson.* **78,** 186–191.
27. Ann, Q., and Adams, J. (1993) Structure-specific collision-induced fragmentations of ceramides cationized with alkali-metal ions. *Anal. Chem.* **65,** 7–13.
28. Olling, A., Breimer, M. E., Samuelsson, B. E., and Ghardashkhani, S. (1998) Electrospray ionization and collision-induced dissociation time-of-flight mass spectrometry of neutral glycosphingolipids. *Rapid. Commun. Mass Spectrom.* **12,** 637–645.
29. Levery, S. B., Toledo, M. S., Straus, A. H., and Takahashi, H. K. (2000) Comparative analysis of ceramide structural modification found in fungal cerebrosides by electrospray tandem mass spectrometry with low energy collision-induced dissociation of Li^+ adduct ions. *Rapid. Commun. Mass Spectrom.* **14,** 551–563.
30. Gorin, P. A. J. (1981) Carbon-13 nuclear magnetic resonance spectroscopy of polysaccharides. *Adv. Carbohydr. Chem. Biochem.* **38,** 13–104.
31. Khoo, K. H., Dell, A., Morris, H. R., Brennan, P. J., and Chatterjee, D. (1995) Structural definition of acylated phosphatidylinositol mannosides from *Mycobacterium tuberculosis:* Definition of a common anchor for lipomannan and lipoarabinomannan. *Glycobiology* **5,** 117–127.
32. Jennemann, R., Bauer, B. L., Bertalnffy, H., Geyer, R., Gschwind, R. M., Selmer, T., and Wiegandt, H. (1999) Novel glycoinositolphosphosphingolipids, basidiolipids, from *Agaricus. Eur. J. Biochem.* **259,** 331–338.
33. Jennemann, R., Geyer, R., Sandhoff, R., Gschwind, R. M., Levery, S. B., Grone, H.-J., and Wiegandt, H. (2001) Glycoinositolphosphosphingolipids, basidiolipids, of higher mushrooms. *Eur. J. Biochem.*, in press.
34. Dickson, R. C., Nagiec, E. E., Skrzypek, M., Tillman, P., Wells, G. B., and Lester, R. L. (1997) Sphingolipids are potential heat stress signals in *Saccharomyces. J. Biol. Chem.* **272,** 30196–30200.
35. Dickson, R. C., and Lester, R. L. (1999) Metabolism and selected functions of sphingolipids in the yeast *Saccharomyces cerevisiae. Biochim. Biophys. Acta* **1438,** 305–321.
36. Beeler, T. J., Fu, D., Rivera, J., Monaghan, E., Gable, K., and Dunn, T. M. (1997) *SUR1* (*CSG1*/*BCL21*), a gene necessary for growth of *Saccharomyces cerevisiae* in the presence of high Ca^{2+} concentrations at 37°C, is required for mannosylation of inositolphosphorylceramide. *Mol. Gen. Genet.* **255,** 570–579.